UDK 591.111.2:543.456
Original scientific article/Izvirni znanstveni članek

ISSN 1580-2949
MTAEC9, 57(5)525(2023)

HEMOCOMPATIBILITY STUDIES OF LAYER-BY-LAYER POLYELECTROLYTE COMPLEXES FOR BIO-BASED POLYMERS

ŠTUDIJ HEMOKOMPATIBILNOSTI VEČPLASTNIH POLIELEKTROLITNIH KOMPLEKSOV ZA BIOPOLIMERE

Mthabisi Talent George Moyo[1,2], Terin Adali[2*], Oğuz Han Edebal[3], Ece Bayir[5,6], Aylin Şendemir[4]

[1]Department of Biomedical Engineering, Faculty of Engineering, Near East University, P.O. Box: 99138, TRNC, Mersin 10 Turkey
[2]Department of Medical Biochemistry, Faculty of Medicine, Girne American University, P.O. Box: 99320 Karaman Girne, Turkish Republic of Northern Cyprus (TRNC), Mersin 10 Turkey.
[3]Clinical Biochemistry Laboratory, Near East University Hospital, P.O. Box: 99138, Turkish Republic of Northern Cyprus (TRNC), Mersin 10 Turkey
[4]Department of Bioengineering, Faculty of Engineering, Ege University, Bornova, 35100 Izmir, Turkey

Prejem rokopisa – received: 2023-07-02; sprejem za objavo – accepted for publication: 2023-08-16

doi:10.17222/mit.2023.922

Thrombogenesis is an important issue that causes failure in blood-contacting biomedical devices. This study focuses on hemocompatibility studies of novel, blood-contacting, polyelectrolyte complexes (PECs) for biomedical application designs. PEC films were fabricated from bio-based polymers of silk fibroin (SF), chitosan (CH), and sodium alginate (AL) through the solvent-casting method as well as the layer-by-layer (LbL) technique. Characterization was carried out by Fourier-transform infrared spectroscopy (FTIR), scanning electron microscopy (SEM), atomic force microscopy (AFM), and differential scanning calorimetry (DSC). FTIR spectra displayed all the layers' characteristic peaks of SF, CH, and AL. AFM images indicated that the addition of AL as an outer layer increased the surface roughness. DSC analysis suggested that the best thermal stability was observed with the CH outer layer of PECs. SEM micrograph analysis indicated that the morphologies of the PECs were affected by the inclusion of the clopidogrel bisulfate (CLB). Hemocompatibility properties were investigated by a complete blood count (CBC), prothrombin time (PT), international normalized ratio (INR), activated partial thromboplastin time (APTT), platelet adhesion, erythrocyte morphology analysis, *in vitro* cholesterol, and albumin level tests. These hemocompatibility analyses demonstrated that the PEC surfaces provide favourable principles to design and develop non-thrombogenic PECs for blood-contacting biomedical applications.

Keywords: polyelectrolyte complex, hemocompatibility, thrombogenesis

Trombogeneza je pomemben pojav, ki povzroča poškodbe na biomehanskih napravah v stiku s človeško krvjo. V študiji, ki je opisana v tem članku so se avtorji osredotočili na raziskavo novih polielektrolitnih kompleksov v stiku s krvjo (PECs, angl.: blood-contacting polyelectrolyte complexes) uporabnih za biomedicinske aplikacije. PEC filme so izdelali iz biopolimerov na osnovi svilenih vlaken (SF, angl.: silk fibroin), hitozana (CH) in natrijevega alginata (AL) s pomočjo tehnike litja raztopine plast za plastjo (LbL; angl.: Layer-by-Layer). Karakterizacijo so izvedli s Fourierjevo transformacijsko spektroskopijo (FTIR), vrstično elektronsko mikroskopijo (SEM), mikroskopijo na atomsko silo (AFM) in vrstično diferencialno kalorimetrijo (DSC). FTIR spekter je prikazal karakteristične spektre vseh plasti SF, CH in AL. AFM slike so pokazale, da dodatek AL poveča površinsko hrapavost zunanje plasti. DSC analiza nakazuje, da ima najboljšo termično stabilnost zunanja plast PEC na osnovi CH. Medtem ko je SEM mikrografska analiza pokazala, da so na morfologije polielektrolitnih kompleksov vplivali vključki klopidogrel bisulfata (CLB). Hemokompatibilnostne lastnosti so določili s kompletnim številom krvi (CBC, angl.: complete blood count), protrombinskim časom (PT), internacionalnim normaliziranim razmerjem (INR), aktiviranim parcialnim časom tromboplastina (APTT), adhezijo ploščic, analizo morfologije eritrocitov, *in vitro* holesterola in testom albuminskega nivoja. Te analize so pokazale, da površine PEC zagotavljajo osnovne ziroma prednostne principe dizajna ter razvoja netrombogenskih polielektrolitnih kompleksov za biomedicinske aplikacije v stiku s krvjo.

Ključne besede: polielektrolitni kompleks, hemokompatibilnost, trombogeneza

1 INTRODUCTION

Hemocompatibility is a challenging problem in blood-contacting biomaterial applications.[1] These non-physiological materials can trigger adverse hematological responses and reactions such as thrombogenicity, embolisms, and blood-related, medical device failure etc.[2] Polyelectrolyte complexes (PECs) have been widely used as films in implants and other therapeutic blood-contacting applications.[3] PECs are a promising approach to the urgent need for designing blood-contacting polymeric applications that have controlled thrombogenic effects.[4]

Thrombogenesis can be activated on any polymeric surface, so elucidating the correlation between material properties and their effect on thrombogenic mechanisms is vital for surface chemistry and biomaterial research. The pursuit of improving hemocompatibility on PEC materials is essential. However, it remains a challenge.[5]

Current approaches for developing hemocompatible PEC surfaces are being investigated and they aim to improve anti-thrombogenesis and control protein adsorption.[6] A study employed the LbL casting technique to

*Corresponding author's e-mail:
terin.adali@neu.edu.tr (Terin Adali)

fabricate Chitosan-poly (γ-glutamic acid) biomaterials for the reduction of protein adsorption and enhance the biocompatibility of the biomaterial.[7] Another study used the same LbL solvent-casting method to fabricate SA/CH films for use as transdermal antihistamine drug-delivery patches.[8] Following the success of this trend, a LbL spraying technique to fabricate biomedical coatings from Poly(L-lysine)–hyaluronan was found to be successful in fabricating hemocompatible biomaterials.[9] After multiple trials, the LbL solvent-casting method was used to generate hydrogel films for wound-healing applications using CH/Heparin sodium.[10]

These complexes are formed when electrostatic interactions between polyanionic and polycationic biopolymers bond each layer compactly.[11] LbL assembly is a distinctive method that employs either dipping, spinning, solvent-casting, electromagnetic, or spraying techniques for the formation of custom PEC films with adjustable properties.[12] The advancement of blood-contacting materials design through the LbL technique is a potential approach to overcoming thrombogenicity and therefore improving its favorable effect on hemocompatibility.[13] Hemocompatibility and material-surface morphology have a strong and direct correlation based on the type of polymer used.[14]

LbL casting is used to modify the surface chemistry of biomaterials by alternatively depositing and adsorbing polyanionic and polycationic biopolymers onto a substrate.[15] Oppositely charged materials used as co-polymer materials have low protein fouling, which has the potential to improve the biocompatibility.[16]

Blood biocompatibility was more achievable in natural-based polymers such as silk fibroin (SF), sodium alginate (AL), and chitosan (CH).[17–21] These bio-based polymer candidates have the potential for remarkable hemocompatibility when cast using the LbL technique. Tailoring these PECs by using the anti-thrombogenic drug may prove to be just as noteworthy. To the best of our knowledge, hemocompatibility studies on tri-layer PEC films prepared by bio-based polymers SF, CH, and AL for use as blood-contacting materials have not been investigated. The novelty of their potential non-thrombogenic and nonhemolytic properties is the point of our interest.

CLB is an anti-thrombogenic agent that decreases the risk of strokes and heart attacks in patients with clotting diseases or patients prone to (or that suffered recent) strokes or heart attacks.[22] Its metabolites inhibit platelet aggregation by binding to the receptors of adenosine diphosphate (ADP), a platelet agonist that causes platelet shape change and aggregation.[23,24] Chemically it is methyl (+) -(S)-α-(2-chlorophenyl)-6,7-dihydrothieno [3,2-c] pyridine-5(4H)-acetate sulfate as seen in CLB has the potential of being used widely in the surface modification of biomaterial design to improve their anti-thrombogenic properties. However, based on a literature survey, limited studies have been carried out on it.

Shitole and colleagues aimed to improve the hemocompatibility of nanofibrous scaffolds, polyurethane/polyethylene glycol scaffolds by incorporating CLB as an anti-thrombogenic treatment. The results of the hemocompatibility assessment indicated that CLB-treated scaffolds demonstrated excellent hemocompatibility, exhibiting lower hemolysis, increased albumin, and plasma protein adsorption, while a reduction in fibrinogen adsorption was noted. Further, the platelet adhesion was highly suppressed and a significant increase in the coagulation period was observed for CLB incorporated scaffolds.[25]

Da Câmara et al. prepared LBL PEC and improved their anti-thrombogenicity by treating them with chondroitin sulfate and glycosaminoglycans heparin. Although this study was effective in proving hemocompatibility, other blood factors like erythrocyte morphology and CBC were not carried out.[26]

Xi et al. fabricated heparin-lysozyme polyelectrolyte multilayers to immobilize on the poly (propylene carbonate) surface by LbL assembly with the aim of hemocompatibility improvement. Combined with the impressive results of platelet adhesion, erythrocyte adhesion, and hemolysis, it was concluded that poly(propylene carbonate)-heparin-lysozyme could be a candidate scaffold material for blood-vessel-tissue engineering due to its high hemocompatibility.[27]

Liu et al. developed a paclitaxel/chitosan LbL nanofiber coating, fabricated with phosphorylcholine groups to improve its hemocompatibility. Their results showed that LbL coatings containing phosphorylcholine groups reduced the platelet adhesion by 6 % and reduced bovine albumin and fibrinogen adsorption by 30–40 %. These results demonstrate that the preparation of the anti-thrombogenic-modified coatings is a simple strategy to improve the hemocompatibility of the polymer complex coatings, has good potential for application in blood-contacting materials and devices.[28]

Manabe and Nara developed LbL elastic multilayer film complexes and deposited them on the hydrophilic surfaces of blood-contacting medical devices to improve their hemocompatibility by suppressing platelet and protein adhesion. The results demonstrate the possibility of coating biomedical multilayer films onto the surface of medical devices.[29]

The objective of this research is to investigate and compare the hemocompatibility properties of PECs assembled using the LbL solvent-casting technique as potential materials to be used as non-thrombogenic, blood-contacting PECs. The characterization of PECs, and the morphological, physicochemical, and biological properties were analyzed.

2 EXPERIMENTAL PART

2.1 Materials

Bombyx Mori Silk cocoons were acquired from Lapta, a town in North Cyprus. Medium-molecular-weight CH with an 85 % deacetylation degree and 200 mPa viscosity in 0.1-M acetic acid at 20 °C, (Fluka) as stated by the producer, was used as supplied. Acetic acid (CH3COOH, Aldrich, Germany), calcium chloride ($CaCl_2$, Aldrich, Germany), sodium carbonate (Na_2CO_3, Aldrich, Germany), methylene bisacrylamide ($C_7N_{10}N_2O_2$, Aldrich, Germany), and ethanol (C_2H_5OH, Aldrich, Germany) were used without further purification. Dialysis membrane (cut off M. W. 12,400) with full average 4 diameters 16 mm and flat width 25 mm capacity of č60 mL/ft was purchased from Aldrich AL (from brown algae Macrocystis pyrifera, medium viscosity) was purchased from Aldrich, Germany. Human venous blood was obtained from the Near East University Hospital. Clopidogrel Bisulfate ($C_{16}H_{18}C_lNO_6S_2$, Aldrich, Germany). All other reagents were of analytical grade and purchased from Aldrich.

2.2 Silk Fibroin Purification

The degumming process was carried out by adding 2g of SF cocoons in a 0.1-M sodium carbonate solution at 75 °C on a magnetic hot-plate stirrer at a speed of 1.5 min^{-1} for 6 h. The degummed silk was washed and rinsed thoroughly with deionized water twice after a 3-hour interval. The degummed silk fibers were dried overnight at room temperature.

2.3 Dissolution and Dialysis of Silk Fibroin

On a continuously stirring magnetic hot plate, the degummed SF fibers were dissolved in a strong electrolyte solution of nC_2H_5OH:nH_2O:$nCaCl_2$ (2: 8: 1) molar ratio at 75 °C. After 3 d of dialysis in deionized water, the aqueous SF solution was obtained, followed by filtration.

2.4 Dissolution of Chitosan

The aqueous CH solution was prepared at a 2 % (w/v) concentration and dissolved in 0.1-M acetic acid solution aided by a magnetic stirrer.

2.5 Dissolution of Sodium Alginate

An aqueous AL solution was prepared with a concentration of 2 % (w/v) by adding AL to deionized water and spun until total dissolution.

2.6 Drug Loading

CLB was dissolved 51mg/L in deionized water. For every 1 mL of aqueous biopolymer used in the PEC film layering, 3 mg of the dissolved CLB was infused.

2.7 Assembly of LbL PEC Films

The solvent-casting method was used to prepare eighteen different compositions of PEC films using SF, CH, and AL in glass Petri dishes (5 cm diameter). These oppositely charged biopolymers were cast LbL to assemble a net-charged polyelectrolyte complex. The desired ultrathin LbL films were obtained by alternating the layering of the oppositely charged polymers. Next, 2.5 mL of aqueous biopolymer was drawn into a sterile syringe and discharged onto a sterile glass petri dish then spread evenly across the surface by rotating in dipped circular motions. Each layer was left to dry for 24 h at room temperature. Extraction of the PECs was followed by washing in methylene bisacrylamide.

2.8 Swelling Kinetics

All the PECs were sampled 2 cm × 2 cm and were investigated by using acetic buffer solution (ABS, pH 4.2), which mimics the pH of healthy wound exudate and phosphate buffer solution (PBS, pH 7.4) that emulates the pH of human venous, arterial and heart capillary blood. The swelling ratios calculated by equation 1:

$$\text{Swelling Ratio } (\%) = \left(\frac{weight_s - weight_{dry}}{weight_{dry}} \right) \times 100\ \% \quad (1)$$

2.9 Differential Scanning Calorimetry (DSC)

Thermoanalysis was performed by utilizing TA Instruments Q20 DSC system to additionally affirm drug-polymer interaction and the mechanical state of PEC. The heating rate was set to 10 °C/min at 25–450 °C, nitrogen flow 50.0 mL/min, 0.2–1 mg samples on an aluminum Hermetic pan.

2.10 Scanning Electron Microscopy (SEM)

The microstructural characterization was made with a Thermo Scientific Apreo S using the secondary-electron in lens method, which is used for high-magnification zoom. The morphologies of the dried samples were analyzed with SEM after being sputter-coated with 7 nm of Au/Pd.

2.11 Atomic Force Microscopy (AFM)

AFM utilizing the BRUKER dimension edge instrument using the tapping mode was used to examine the surface geology and topography.

2.12 Fourier-Transform Infrared Spectroscopy (FTIR)

Analysis was carried out using a PerkinElmer FTIR spectrometer with an attenuated total reflection (ATR) function to take the measurements within the range 600–4000 cm^{-1}.

2.13 In-vitro Hemocompatibility Assay

At the Near East University hospital, fresh human whole blood samples were obtained from a healthy male donor by venipuncture using the vacuum blood-collection system into 2 mL anticoagulated collecting tubes. Two different evacuated tubes were used, one contained 3.6 mg K_2EDTA as an anti-coagulant, and the other contained 3.2 % sodium citrate. *In vitro* anticoagulation tests, total cholesterol and albumin analysis, *in vitro* platelet adhesion, and erythrocyte morphology analysis were effective tests to determine the hemocompatibility of PECs according to the ISO 10993. For the mentioned hemocompatibility analyses, the anticoagulated tubes were centrifuged at 1500 min^{-1}, 15 min for an investigation of each blood-compatibility assay. A CBC analysis was obtained by using uncentrifuged blood and all the anticoagulated blood was used within 1 h of collection. For the analysis of the platelet adhesion and erythrocyte morphology, PEC-A, PEC-C, PEC-D, PEC-E, PEC-1, PEC-3, PEC-4, PEC-5 were used as test samples, while PECs PEC-1, PEC-5, PEC-A, and PEC-E were used as test samples to evaluate the *in-vitro* anticoagulation tests, total cholesterol, and albumin analysis and CBC.

2.13.1 In-vitro Anticoagulation Analysis

For the evaluation of baseline coagulation and material-blood contacted parameters utilizing the STA Compact and fresh venous blood, the blood samples were anticoagulated in sample collection tubes containing 3.2 % sodium citrate at blood to an anticoagulant ratio of 9:1 (v/v). A plasma sample was used to measure the activated partial thrombin time (APTT) and the prothrombin time (PT) of the material contacting blood as blood-clotting tests using cephascreen and stago STA-Neoplastine CI Plus commercial reagents. Platelet-rich plasma (PRP) was subsequently transferred to sterile test tubes containing the biomaterials under study and incubated at 37 °C for 60 min. The international normalized ratio (INR) was investigated using equation 2; the international sensitivity index (ISI) as a thromboplastin referencing model to liken all thromboplastins performed. INR depends on the proportion of the patient's prothrombin time and the typical mean prothrombin time.

$$\mathrm{INR} = \left(\frac{\text{patient PT}}{\text{mean normal PT}} \right)^{\mathrm{ISI}} \qquad (2)$$

where ISI is the international sensitivity index of the thromboplastin tested

2.13.2 Total Cholesterol & Albumin

Platelet-rich plasma was placed into a separate Eppendorf tube containing the test biomaterial then incubated at 37 °C for 15 min and further shaken on a KS 260 basic flat orbital shaker at 300 min^{-1} for 20 min. After shaking the biomaterials were recovered from the serum and the suspension-free serum samples were tested for total cholesterol and albumin using a biochemistry autoanalyzer (Abbott Architect, Abbott Laboratories, Diagnostic Division, Abbott Park, IL).

2.13.3 Complete Blood Count (CBC)

For 30 min, specimens submerged in whole blood were shaken at 300 min^{-1} at room temperature. Complete blood count (erythrocytes, leukocytes, and platelets) of all PEC-contacting and non-PEC-contacting blood samples was determined using a hematology analyzer (Cell Dyn Ruby hematology analyzer Abbott Laboratories, Diagnostic Division, Abbott Park, IL).

2.13.4 In-vitro Platelet Adhesion

PEC samples were incubated in fresh human PRP for 15 min within static conditions at 37 °C and further shaken on a KS 260 basic flat orbital shaker at 300 min^{-1} for 20 min at room temperature. After shaking, the biomaterials were recovered from the serum and the suspension-free serum samples were repeatedly washed in ultra-pure water, after which the direct-drying technique was used with May Grünwald and Giemsa dye. The peripheric screening technique was employed to determine the degree of PEC surface-platelet adherence. Light microscopy was utilized for the investigation of the platelet microparticle formation, amount, adhesion, and morphology. All samples were investigated at 400× magnification (450 μ).

2.13.5 Erythrocyte Morphology Analysis

Erythrocyte membrane integrity analysis was carried out to investigate any abnormalities of their shape after RBC contact with the PECs. Biomaterial contacting RBC test tubes were shaken at 300 min^{-1} for 20 min then incubated at 37 °C for 20 min. Peripheral blood smears were stained using the standard Wright-Giemsa Stain Method where the specimen was fixated onto the slides with alcohol. The smears were examined at 400 × magnification (450 μ) in 10 different areas.

3 RESULTS

3.1 Derived LBL PEC Film Compositions

Compositions of the assembled PEC films are detailed in **Table 1**.

Table 1: Compositions of derived PEC films

Sample	Composition	Sample	Composition
Drug loaded		Drug-free	
PEC-A	CH/SF/CH + clb	PEC-1	CH/ SF/CH
PEC-B	SF/CH + clb	PEC-2	SF/CH
PEC-C	SF/CH/SF +clb	PEC-3	SF/CH/SF
PEC-D	AL/CH/SF + clb	PEC-4	AL//CH/SF
PEC-E	AL/SF/AL+ clb	PEC-5	AL/SF/AL
PEC-F	SF/AL + clb	PEC-6	SF/AL
PEC-G	SF + clb	PEC-7	SF
PEC-H	CH + clb	PEC-8	CH
PEC-I	AL + clb	PEC-9	AL

3.2 Swelling Kinetics

Table 2 compares the swelling ratios of the films based on two solvents with different polarities, where all the swelling behaviour is plotted for an average of three trials.

Table 2: Optimal swelling ratio (SR%) of PECs in ABS and PBS

	ABS: pH 4.2		PBS: pH 7.4	
Sample	Time (min)	S.R%	Time	S.R%
PEC-A	35	190.78	15	197.33
PEC-B	10	89.62	10	181.95
PEC-C	10	210.37	20	213.9
PEC-D	10	455.78	35	564.87
PEC-E	5	602.3	55	1253.65
PEC-F	10	109.52	80	188.66
PEC-G	15	52.66	10	131.21
PEC-H	10	51.49	55	108
PEC-I	20	60.53	35	156.66
PEC-1	55	118.26	55	131.21
PEC-2	35	69.05	35	106.66
PEC-3	10	148.53	10	151.44
PEC-4	20	197.33	20	198.66
PEC-5	10	265.7	10	257.33
PEC-6	10	72.85	10	108
PEC-7	10	55.34	10	76.33
PEC-8	25	52.36	25	74.66
PEC-9	15	68.45	15	84.97

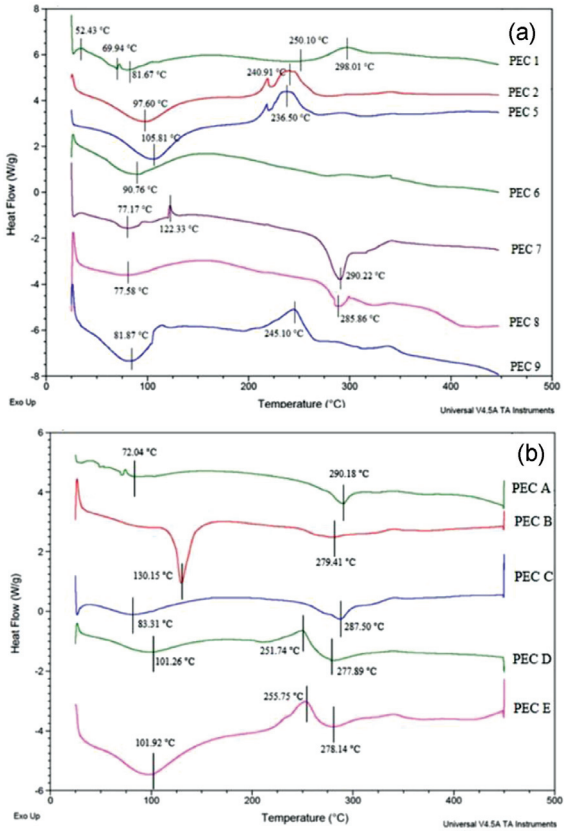

Figure 1: DSC analysis of (A) drug-free films and (B) drug-loaded films

3.3 Differential Scanning Calorimetry (DSC)

Figure 1 shows analytical differences of the DSC thermograms of all PECs.

3.4 Atomic force microscopy (AFM)

Topologies of 8 PEC films were used in the AFM analysis. **Figure 2** displays the differences in the topographic features of samples PEC-1, PEC-3, PEC-4, PEC-5, PEC-A, PEC-C, PEC-D, PEC-E. In this study, PEC-3 recorded minimum roughness as Ra = 9.1 nm and maximum roughness in PEC-E as Ra = 113 nm.

3.5 Scanning Electron Microscopy (SEM)

The SEM micrographs of all the PECs presented in **Figure 3** show their differences in topographic features.

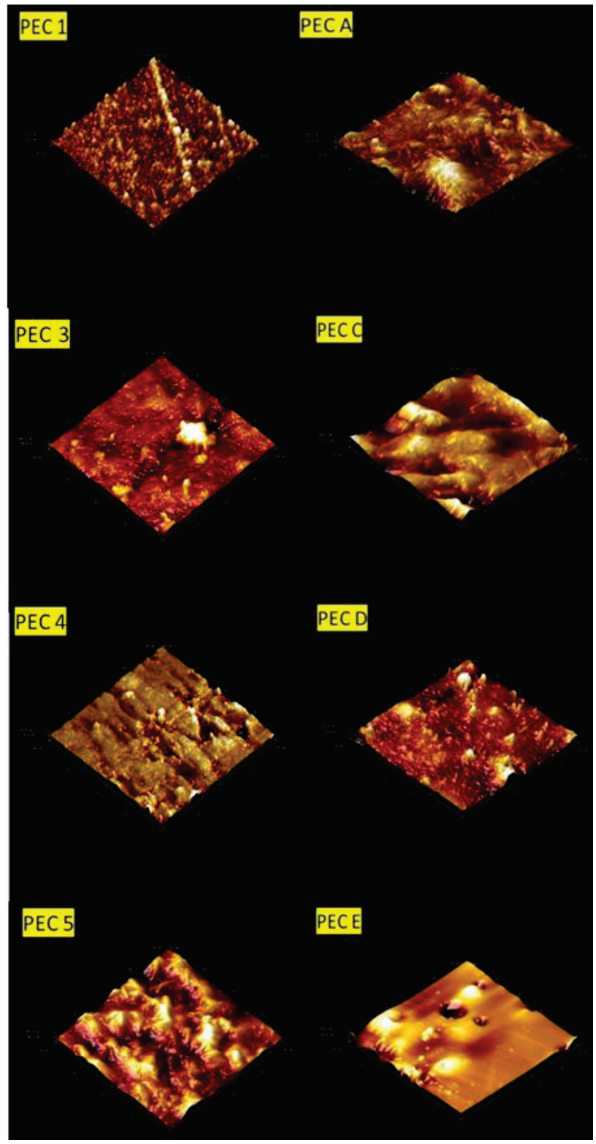

Figure 2: 3D AFM thermograms of PEC-1, PEC-3, PEC-4, PEC-5, PEC-5, PEC-A, PEC-C, PEC-D, PEC-E

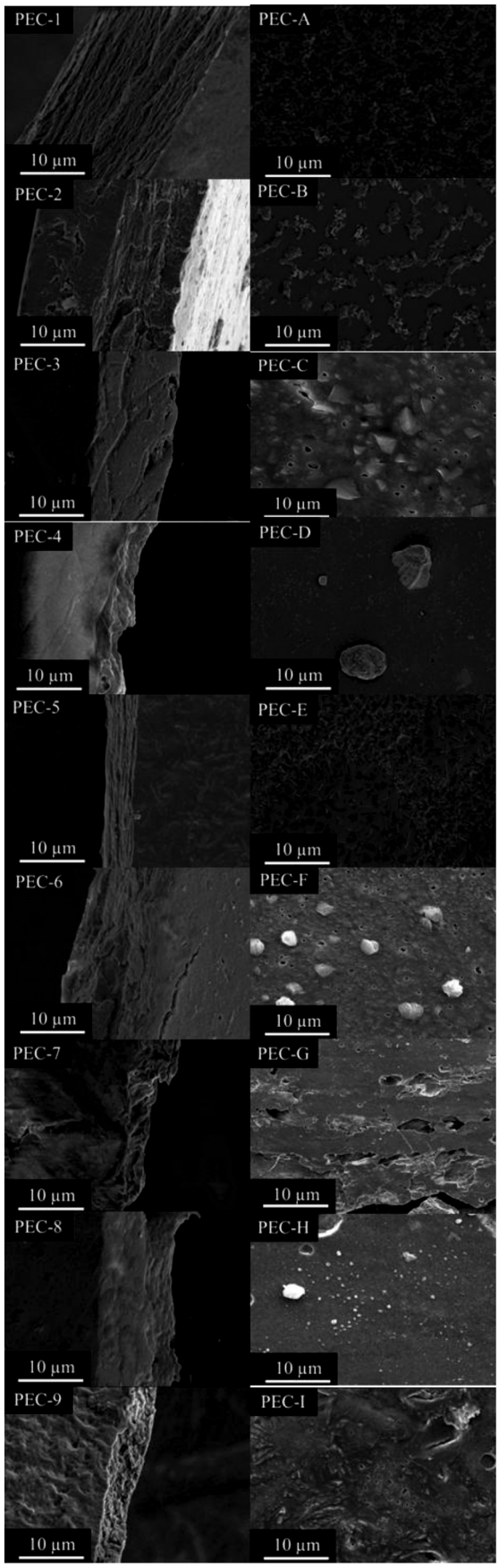

Figure 3: SEM images of drug-free and drug-loaded PECs at 10 µm

Drug-free PEC without AL appears smooth, while the CLB addition changed the morphology according to PEC A, PEC-B and PEC-E.

3.6 Fourier-Transform Infrared Spectroscopy (FTIR)

The FTIR spectra are shown in **Figure 4a** for drug-loaded and **Figure 4b** for drug-free biomacromolecules.

3.7 In-vitro Anticoagulation, Cholesterol and Albumin

Table 3 displays the results of the PT, APTT, and INR values for the control (blood without sample) and test specimen after incubation. Additionally, it displays the results of the blood cholesterol and albumin analyses of PEC-1, PEC-5, PEC-A, and PEC-E. **Table 3a** shows that PT, PTT, and INR values for the blood in contact with PECs are shorter than the control, indicating that PECs might activate the coagulation process. **Table 3b**

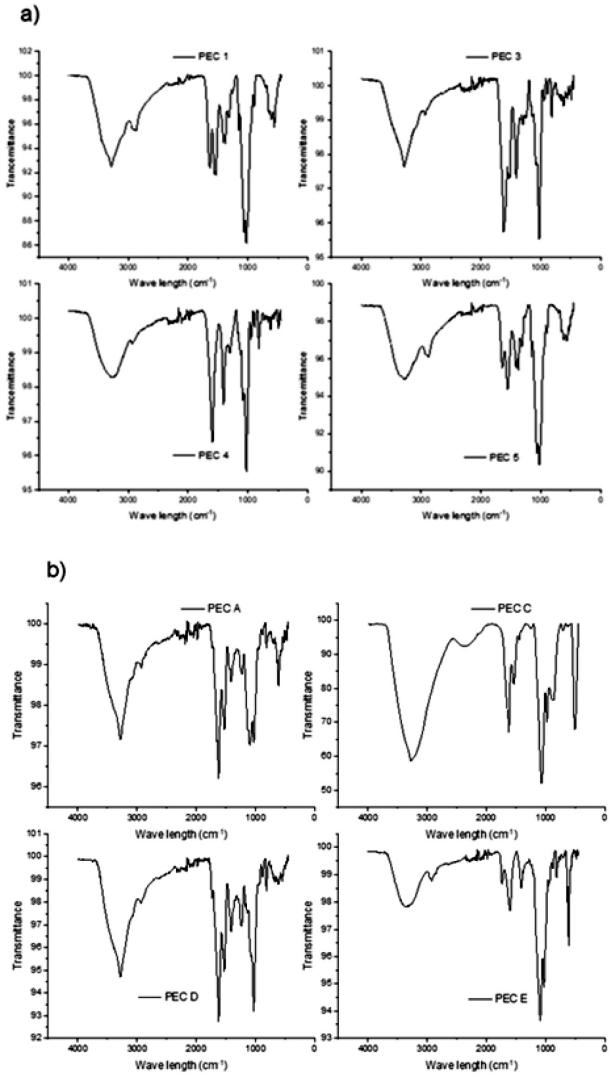

Figure 4: a) FTIR results of drug-free films PEC 1, **b)** drug-loaded films PEC A – I

shows that cholesterol and albumin efflux saturation in all PECs were within range.

Table 3: a)Anticoagulation analysis of PEC-1, PEC-5, PEC-A, and PEC-E, b) Blood cholesterol and albumin analysis of PEC-1, PEC-5, PEC-A, and PEC-E

a)				
Sample	INR	PT (%)	PT (Sec)	APTT (sec)
Control	1.34	65	17.6	31.8
PEC-1	1.09	88	14.4	32.7
PEC-5	1.17	79	15.4	86.1
PEC-A	1.11	85	14.7	57.7
PEC-E	1.07	90	14.2	101.4
b)				
Sample	Cholesterol range (mg/dL)	Cholesterol (mg/dL)	Albumin range (g/dL)	Albumin (g/dL)
Control	200	189	3.4–5.4	5.1
PEC-1	200	182	3.4–5.4	4.8
PEC-5	200	176	3.4–5.4	4.5
PEC-A	200	172	3.4–5.4	4.1
PEC-E	200	185	3.4–5.4	4.9

PT: Prothrombin Time, INR: International Normalized Ratio, APTT: Activated Partial Thromboplastin Time

3.8 Complete Blood Count (CBC)

Table 4: Complete blood-count analysis of PEC-1, PEC-5, PEC-A, and PEC-E

		Samples				
Parameters	Range	Con-trol	PEC-1	PEC-5	PEC-A	PEC-E
WBC (10e3/uL)	3.70–10.1	4.15	4.39	4.30	4.02	4.20
NEU (%)	1.63–6.96	2.25	2.33	2.17	2.13	2.31
LYM (%)	1.09–2.99	1.41	1.54	1.55	1.52	1.47
MONO (%)	0.240–0.790	.385	.414	.365	.290	.395
EOS (%)	0.030–0.440	.042	.048	.055	.062	.065
BASO (%)	0.00–0.080	.061	.058	.055	.021	.063
RBC (10e6/uL)	4.06–4.69	5.92	5.87	5.99	6.21	6.00
HGB (g/dL)	11.0–16.0	17.1	17.2	17.8	18.3	18.0
HCT (%)	37.7–53.7	51.5	51.2	52.2	54.1	52.0
MCV (fL)	81.1–96.0	86.9	87.2	87.0	87.1	86.6
MCH (pg)	27.0–31.2	28.9	29.3	29.7	29.4	30.0
MCHC (g/dL)	31.8–35.4	33.3	33.6	34.1	33.8	34.6
RDW (%)	11.5–14.5	12.0	11.9	11.9	12	11.9
PLT (10e3/uL)	155–366	342	335	337	335	319
MPV (fL)	6.90–10.6	6.41	6.63	6.77	6.78	6.63

The hematology analyzer uses a spectrophotometric method for hemoglobin measurement. The CBC results are shown in **Table 4**.

3.9 In-vitro Platelet Adhesion Analyses with Peripheric Smear Test

The light micrograph demonstrated that no thrombi adhere to the surface of the biomaterials, as shown in

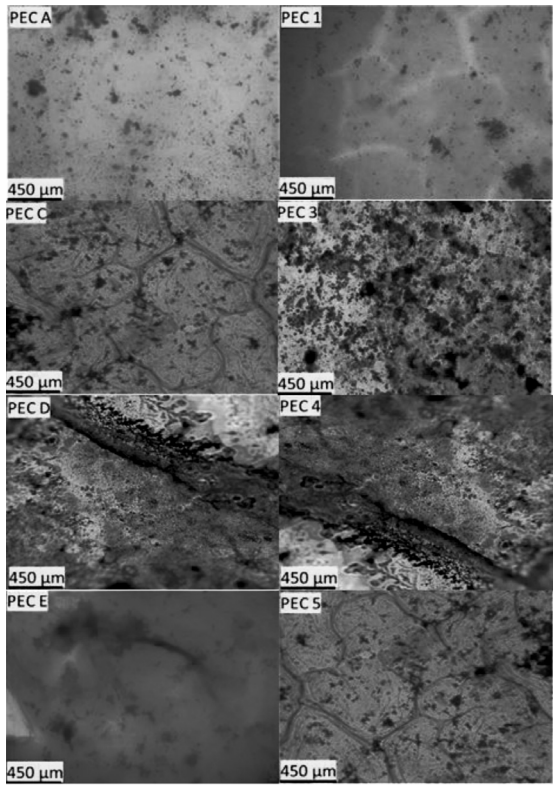

Figure 5: Peripheral blood smears for platelet-adhesion analysis of PEC-1, PEC-3, PEC-4, PEC-5, PEC-A, PEC-C, PEC-D, PEC-E at 450 µm

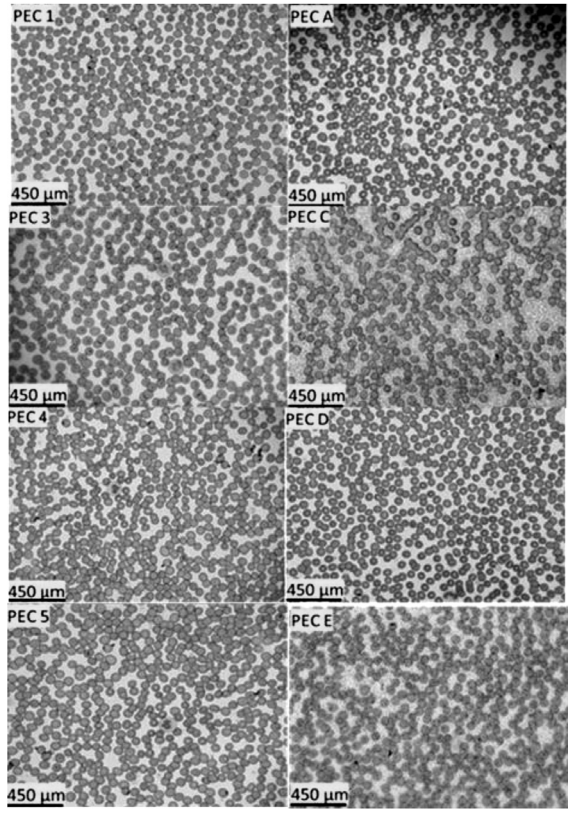

Figure 6: Wright-Giemsa Stains of PEC-1, PEC-3, PEC-4, PEC-5, PEC-A, PEC-C, PEC-D, PEC-E at 450 × magnification for erythrocyte morphology analysis

Figure 5. The results indicated that the drug-loaded and drug-free PECs could be considered ideal candidates for biomedical applications. No signs of platelet aggregation; however, the biomaterials were very densely stained.

3.10 Erythrocyte Morphology Analysis

Direct hemolysis testing was performed as shown in **Figure 6.** No morphological changes in erythrocytes were noted except in PEC-E, which caused a slight deterioration in the erythrocyte morphology. The erythrocytes physically contacting the surface of biomaterials PEC-A, PEC-1, PEC-3, PEC-4, and PEC-5 exhibited completely normal biconcave morphology.

4 DISCUSSION

We would like to acknowledge that there is missing data in our study. During the data-collection process, we encountered technical and financial difficulties with the measurement equipment, which resulted in incomplete data for some variables. Despite our efforts to address these issues promptly, we were unable to recover the missing data. However, it is important to note that the variables consistent with all the experimental analysis are PEC-1, PEC-5, PEC-A and PEC-E. Overall, the results support the robustness of our main conclusions.

Eighteen PEC samples with the intended use as blood-contacting biomaterials were fabricated using the LbL casting technique. Drug-loaded and drug-free PECs were evaluated in various characterization and hemocompatibility assays to investigate the effect of electrostatic interaction and surface modification using CLB as an anti-thrombogenic agent.

The water-absorption capacity of a biomaterial is an important factor when it is applied as a transdermal patch for wound healing or wound dressing. A biomaterial with excellent water-absorbing properties absorbs exudates and keeps the wound dry, thereby conserving a proper moist environment that stimulates optimal wound healing.[30] In this experiment, PECs absorbed the solvent solution until the maximum swelling was achieved; thereupon the degree of swelling dropped, after which they shrank and degraded. Out of the three biopolymers, the literature suggested that AL has the highest swelling capacity attributed to its randomly distributed hydrophilic units on its polymeric chain.[31] AL has a higher swelling capacity than SF because SF has hydrophobic chains in its backbone. The heavy (H) chain with hydrophobic domains attributes its lower swelling ratio, but remains higher than CH.[32] Literature has shown that of the three biopolymers, CH is the least hydrophilic due to its net positive charge assimilating hydrophobic chains.[33] The highest swelling ratio of 1253.65 % was seen in PEC-E at pH 7.2. This high swelling ratio is attributed to the net negative charge of the hydrophilic biopolymer's SF and AL. AL as an outer layer of the tri-layer PEC has more hydrophilic chains than SF, thus retaining a greater amount of solvent in its polymer chains. The swelling ratio decreased gradually with the number of hydrophilic groups present in the complex. The lowest swelling ratio of 51.49 % was in PEC-H in pH 4.2, which is comprised of CH only. This result is parallel to a study by Liwe et al., where PEC films containing AL exhibited excellent swelling characteristics, a lot more CH.[34]

The amount of absorbed solvent is closely correlated with the number of hydroxyl groups present in the PEC film structure. Hydroxyl groups are responsible for the formation of hydrogen bonds with water molecules. Generally, the solvent-uptake capacity increases by adding a hydrophilic component. In this study, a highly hydrophilic component, i.e., AL, was added to increase the swelling capacity of the PEC films. The improvement in the PEC film swelling ratio with the increase in the AL content is mainly attributed to the ionic character of AL. Characterization was carried out to investigate the vitality of the functional groups.

The DSC results suggest that progressively accessible protonated amine groups in CH might bring about carboxylic groups in SF. PEC-B indicated the weakest thermal stability, registered by the least difference in exothermic peaks 130.15 °C and 279.41°C, respectively, among all the peaks. Bond disruption, chain scission, or drug degradation of macromolecules may be a cause of the decrease in thermal stability.[35] An indication of oxidative degradation and hydrogen bonding disruption due to a loss of free-amine groups. Strong molecular interactions and chemical bonds might be present between SF and CH. There were other nucleation sites such as carbonyl (–C–O) and amine (–N–H–) groups on SF molecules besides the carboxyl (–COOH) and hydroxyl (–OH) groups previously reported that were further investigated using AFM.

Topologies of 8 PEC films were used in the AFM analysis. The addition of AL to a complex increases its roughness. The characteristic roughness after the addition of CLB is in PEC-C with a maximum roughness of Ra = 53.6 nm. Thermograms of PEC-A and PEC-E show that the addition of CLB does not increase the surface roughness, which is a favourable trait in this because studies have shown that elevated surface roughness triggers blood protein and platelet aggregation. Another study reported that ionic cross-linking utilizing sulfuric acid altered the heterogenicity of CH as an outer layer.[36] Differences in the topologies were additionally investigated using SEM. Scanning electron microscopy micrographs showed that the increasing number of layers is proportional to PEC thickness, they also showed that the addition of CLB changed the morphology of the biomaterials.

In the FTIR spectrum of pure CH and CH-containing PECs, three specific absorption peaks at about 1034 cm^{-1}, 1602 cm^{-1}, and 3319 appeared, respectively, corre-

sponding to the O-C, C=C stretch, and the sharp C-H stretch. AL displayed similar absorption peaks. Also, three characteristic absorption peaks at 1545 cm^{-1}, 1642 cm^{-1}, and 3299 cm^{-1} were observed in the FTIR spectrum of SF- and SF-containing PECs, which were attributed to double C-C stretching, and sharp, C-H stretching, respectively. A study by Mohammed and Mohammed discovered that the FTIR spectrum of pure CLB showed a strong absorbance band due to C=O stretching vibrations at 1752 cm^{-1} and due to O–H stretching of the hydrogen sulfate moiety around 3012 cm^{-1}. The band due to aromatic C– H stretching vibrations represented at 3121 cm^{-1}.

The FTIR spectrum included also a broad absorbance band at 2505 cm^{-1}, which can be attributed to the stretching vibrations of the bonded N–H resulting from salt formation between the quaternary nitrogen of CLB and –OH of hydrogen sulfate. The FTIR spectra in **Figure 4a** can be attributed to the results of pure CLB spectra due to drug loading of the anti-thrombogenic drug.[37]

The compatibility of the various PEC films with human blood was evaluated by investigating their ability to alter the coagulation times. In this study, for the first time, to the best of our knowledge, we analyzed the effect of electrostatically assembling PEC films prepared by LbL solvent casting for determining the plasma coagulation. According to previous experiments investigating similar parameters, the reference range of PT, APTT and INR are for PT is 11.0–12.5 s; 65–95 % activity (although the normal range depends on reagents used for PT), APTT is 30–40 s and INR is 0.8–1.1.[38–43]

A study conducted by Qing et al. indicated that the positive charges of CH inhibited activation of the contact system and retarded thrombin generation and blood coagulation on the fabricated CH films.[44] Another study conducted by Zhang et al. contradicted these results by reporting that blood coagulation is dependent on the molecular weight and deacetylation degree of CH. The hemostatic effects of CH investigated showed that when the molecular weights were high (105–106) and approximate, the coagulation effect of CH improved with a decrease of the deacetylation degree and achieved a prominent level in a moderate degree of deacetylation (68.36 %). With the same degree of deacetylation, the higher the molecular weight of CH, the better the procoagulant effect.[45] The results obtained in these studies led us to select PEC-1 and PEC-A that are electrostatically charged with CH as its outer layers to test. An additional study by Lihong et al. indicated that introducing sulfate groups could not increase PT, it had little effect on coagulation factors in the extrinsic pathway.[46] For the sake of comparison, we investigated this fact using PEC-5 and PEC-E as samples with AL as an outer layer.

Our present findings improve understanding of the events leading to blood coagulation on films with CH and AL as outer layers, which will be useful for the future development of novel CH and AL-based hemostatic materials. **Table 4** displays the results of the PT, APTT, and INR values for the control (blood without sample) and test specimen after incubation. The PT, PTT, and INR values for the blood in contact with PECs are shorter than the control, indicating that PECs might activate the coagulation process.

An assessment of the change in cholesterol and albumin levels after 60 minutes of contact with samples PEC-1, PEC-A, PEC-5, and PEC-E was investigated to the best our knowledge these parameters have not been investigated before on PECs of this assembly. Total cholesterol levels less than 200 milligrams per deciliter (mg/dL) are considered desirable for adults.[47–50] While the normal range for albumin is about 3.4 g/dL to 5.4 g/dL.[51–53]

A thorough literature survey supports that this analysis has not been carried out on PECs of this nature before. The number of erythrocytes, leukocytes, and platelets was measured before and after the incubation of blood with the biomaterial using a hematology analyzer, which uses flow cytometry. The hematology analyzer utilizes uses a spectrophotometric method for hemoglobin measurement.

An increase in the platelet release or elevated platelet aggregation on the biomaterial surface is a sign of material thrombogenicity.[54] Thrombogenicity refers to the tendency of a material in contact with the blood to produce a thrombus or a clot.[55] A decrease in platelet count over time is indicative of a thrombogenic material and anti-thrombogenic materials reduce the activation of platelets.[56] Material surfaces that remain inert to blood contact are considered non-thrombogenic and are preferred for use in biomedical applications.[57] The platelet count of whole blood-contacting all tested PECs remained within the normal range and close to the control value of 342 (10e3/uL). Whole blood-contacting PEC-1 and PEC-A separately both recorded a platelet reading of 335 (10e3/uL). Within the realms of this study, these results suggest that CH as an outer layer has no significant impact on the level of platelets, nor does the addition of CLB. Of all the tested PECs, whole blood contacting PEC-5 and PEC-E recorded the highest and lowest platelet readings of 337 (10e3/uL) and 319 (10e3/uL) respectively. These findings may indicate that the net negatively charged SF and AL tri-layer PECs with AL as an outer layer have significant effects on thrombogenicity. PEC-5 is drug free and has the highest platelet readings, compared to PEC-E with the exact same composition; however, PEC-E is embedded with the antithrombogenic drug, so in this work CLB lowers the levels of platelets in net negatively charged PECs with AL as an outer layer.

Furthermore, besides thrombogenicity, blood levels of leukocytes were analyzed to evaluate the leukocyte depletion and/or augmentation responses induced by biomaterial contact. The white blood cell count of the whole blood-contacting all the tested PECs remained

within normal range and most of the results remained close to the control reading of 4.15 (10e3/uL). Whole blood-contacting PEC-1, PEC-5, PEC-A and PEC-E were 4.39 (10e3/uL), 4.20 (10e3/uL), 4.02 (10e3/uL) and 4.30 (10e3/uL), respectively. PEC-1 and PEC-A have the same biopolymer composition; however, the PEC-A is embedded with the anti-thrombogenic drug and PEC-1 drug-free. Of all the tested PECs, the whole blood-contacting PEC-1 and PEC-A recorded the highest and lowest white blood-cell readings, respectively. Although there are some slight differences between the whole-blood specimens incubated with biomaterials, these are not significant. It can be said that neither of these biomaterials has any marked impact on the leukocyte levels of the blood.

Polycythemia refers to an abnormal increase in the number of red blood cells. Biomaterials that cause polycythemia increase the risk of other health issues, such as blood clots, stroke, heart disease, etc. The RBC count of all the biomaterial contacting whole blood samples exceeded the normal range. This may be attributed to the donor's high RBC count seeing as the control was 5.92 (10e3/uL) which is above the range. Whole blood-contacting PECs- 1, 5, A, and E were 5.87 (10e3/uL), 5.99 (10e3/uL), 6.21 (10e3/uL) and 6.00 (10e3/uL), respectively. These high readings may be due to the interactions between blood plasma and biomaterial, leading to water being held by the biomaterial and an increased concentration of RBCs.

Understanding the ability of thrombus formation on blood-contacting devices is thought to be crucial because early post-operative platelet adherence might be responsible for the formation of thrombi, which has an adverse postoperative outcome.[58–60] Thus, platelet adhesion is reported to be an early indicator of the thrombogenicity of blood-contacting implants.[61,62] The exposure of biomaterial to the blood can result in an undesired activation of platelets and so lead to thrombotic complications. Thus, the analysis of platelet activation is an important part of the hemocompatibility tests. The contact of blood with foreign surfaces immediately leads to the adsorption of plasma proteins.[63,64]

The *in vitro* peripheric smear test was applied to PRP-immersed biomaterials to analyze their platelet-adhesion properties for evaluating the primary hemostasis of the prepared biomaterials. The PEC-A and PEC-E had dense and diffused staining, which suggests that the biomaterials have a lot of open molecules for chemical bonding with other molecules. Taken together, the interactions of PEC-E with plasma, they do not induce any significant alteration in the cell-membrane structure and function as well as in cell morphology after both the short- and long-term incubation.

Biomaterial interaction with blood may lead to hemolysis, which is accompanied by the release of hemoglobin.[65] Thus, an increased concentration of free hemoglobin in the plasma is a direct indicator of erythrocytes destruction. The damage of erythrocytes can lead to reduced oxygen transport to tissues and organs *in vivo* and increased levels of free hemoglobin can induce toxicity or alter kidney function.[66,67] Thus, hemolysis can be analyzed after direct or indirect blood contact. In direct analysis, blood is incubated with the biomaterial and investigated.[68–70]

The Erythrocytes physically contacting the surface of biomaterials PEC-A, PEC-1 and PEC-5 exhibited completely normal biconcave morphology. Biomaterial PEC-E caused abnormal swelling and deformation of erythrocyte membranes furthermore lots of small strayed particles were observed on the slide.

5 CONCLUSIONS

These layer-by-layer polyelectrolyte complexes are good candidates to be used as blood-compatible biomaterials for biomedical applications. They show minimal to no interaction with blood cells, or plasma proteins, in terms of affecting their blood levels *in vitro*. Further *in-vitro* studies can be carried out with longer incubation periods, or on blood, specimens taken from multiple volunteers.

Acknowledgment

The authors acknowledge the Tissue Engineering and Biomaterials Research Center, Center of Excellence, Near East University, Near East University Hospital, Clinical Biochemistry Laboratory, Central Research Test and Analysis Laboratory Application and Research Center (EGE-MATAL), Ege University, Department of Bioengineering, Faculty of Engineering, Ege University, Bornova, and Sabanci University SUNUM Nanotechnology Research Center.

6 REFERENCES

[1] E. Ozkan et al., Bioinspired ultra-low fouling coatings on medical devices to prevent device-associated infections and thrombosis. Journal of colloid and interface science 608 (**2022**), 1015–1024, doi:10.1016/j.jcis.2021.09.183

[2] P. S. Yavvari et al., Emerging biomedical applications of polyaspartic acid-derived biodegradable polyelectrolytes and polyelectrolyte complexes. Journal of materials chemistry B 7.13 (**2019**), 2102–2122, doi:10.1039/c8tb02962h

[3] C. A. Labarrere, E. D. Ali, S. K. Ghassan Thrombogenic and inflammatory reactions to biomaterials in medical devices. Frontiers in Bioengineering and biotechnology 8 (**2020**), 123, doi:10.1039/c8tb02962h

[4] E. Maretti et al., Chitosan/heparin polyelectrolyte complexes as ion-paring approach to encapsulate heparin in orally administrable SLN: In vitro evaluation. Colloids and Surfaces A: Physicochemical and Engineering Aspects 608 (**2021**), 125606, doi:10.3389/fbioe.2020.00123

[5] I. H., Jaffer, I. W. Jeffrey, The blood compatibility challenge. Part 1: Blood-contacting medical devices: The scope of the problem. Acta biomaterialia 94 (**2019**): 2–10. doi:10.1016/j.colsurfa.2020.125606

[6] M. Hedayati, M. J. Neufeld, M. M. Reynolds, M. J.Kipper, The quest for blood-compatible materials: Recent advances and future technologies. Mater Sci Eng R Rep. 2019; 138 (July):118–152. doi:10.1016/j.mser.2019.06.002

[7] P. K. Panda, J. M. Yang, Y. H.Chang, Preparation and characterization of ferulic acid-modified water soluble chitosan and poly (γ-glutamic acid) polyelectrolyte films through layer-by-layer assembly towards protein adsorption. Int J Biol Macromol., 171, (**2021**), 457–464. doi:10.1016/j.ijbiomac.2020.12.226

[8] S. Lefnaoui et al., Design of antihistaminic transdermal films based on alginate–chitosan polyelectrolyte complexes: characterization and permeation studies. Drug development and industrial pharmacy, 44.3 (**2018**), 432–443. doi:10.1080/03639045.2017.1395461

[9] J. Wang et al., Humidity-Triggered Relaxation of Polyelectrolyte Complexes as a Robust Approach to Generate Extracellular Matrix Biomimetic Films. Advanced Healthcare Materials 9.14 (**2020**), 2000381. doi:10.1002/adhm.202000381

[10] M. Shu et al., High strength and antibacterial polyelectrolyte complex CS/HS hydrogel films for wound healing. Soft Matter 15.38 (20–19), 7686–7694. doi:10.1039/c9sm01380f

[11] B. D. Ippel, P. Y. W. Dankers, Introduction of Nature's Complexity in Engineered Blood-compatible Biomaterials. Adv Healthc Mater., 7 (2018) 1, 1–17. doi:10.1002/adhm.201700505

[12] J. J. Richardson et al. Innovation in layer-by-layer assembly. Chemical reviews 116.23 (**2016**), 14828–14867. doi:10.1021/acs.chemrev.6b00627

[13] M. F. Maitz et al. The blood compatibility challenge. Part 4: Surface modification for hemocompatible materials: Passive and active approaches to guide blood-material interactions. Acta Biomaterialia, 94 (**2019**), 33–43. doi:10.1016/j.actbio.2019.06.019

[14] N. Asadi et al. Common biocompatible polymeric materials for tissue engineering and regenerative medicine. Materials Chemistry and Physics 242 (**2020**), 122528. doi:10.1016/j.matchemphys.2019.122528

[15] R. R. Costa, F. M. Joao Polyelectrolyte multilayered assemblies in biomedical technologies. Chemical Society Reviews 43.10 (**2014**), 3453–3479. doi:10.1039/C3CS60393H

[16] S. Chen, J. Shaoyi, An new avenue to nonfouling materials. Advanced Materials 20.2 (**2008**): 335–338. doi:10.1002/adma.200701164

[17] S. Pahal et al., Polyelectrolyte multilayers for bio-applications: recent advancements. IET nanobiotechnology 11.8 (**2017**), 903–908. doi:10.1049/iet-nbt.2017.0007

[18] M. Uncu, Silk fibroin as a non-thrombogenic biomaterial. International journal of biological macromolecules (**2016**). doi:10.1016/j.ijbiomac.2016.01.088

[19] P. Tulay, G. Nanyak, A. Terin, The wonders of silk fibroin biomaterials in the treatment of breast cancer. Critical Reviews™ in Eukaryotic Gene Expression 28.2 (**2018**). doi:10.1615/CritRevEukaryotGeneExpr.2018021331

[20] T. Adali, Synthesis and characterization of noncytotoxic and biodegradable polymethacrylates-grafted chitosan gels. Bio-Medical Materials and Engineering 23.5 (**2013**), 349–359. doi:10.3233/BME-130759

[21] E. Bahramzadeh, Y. Elvan, T. Adali, Chitosan-graft-poly (N-hydroxy ethyl acrylamide) copolymers: Synthesis, characterization and preliminary blood compatibility in vitro. International journal of biological macromolecules 123 (**2019**), 1257–1266.

[22] Y.-J. Zhang et al., Pharmacokinetic and pharmacodynamic responses to clopidogrel: evidences and perspectives. International Journal of Environmental Research and Public Health 14.3 (**2017**): 301. doi:10.3390/ijerph14030301

[23] Jin, Jianguo, et al. Adenosine diphosphate (ADP)–induced thromboxane A2generation in human platelets requires coordinated signaling through integrin αIIbβ3 and ADP receptors. Blood, The Journal of the American Society of Hematology 99.1 (**2002**), 193–198. doi:10.1182/blood.V99.1.193

[24] S. Ji et al., Segmented scan modes and polarity-based LC-MS for pharmacokinetic interaction study between Fufang Danshen Dripping Pill and Clopidogrel Bisulfate Tablet. Journal of Pharmaceutical and Biomedical Analysis 174 (**2019**), 367–375. doi:10.1016/j.jpba.2019.05.055

[25] A. A. Shitole et al., Clopidogrel eluting electrospun polyurethane/polyethylene glycol thromboresistant, hemocompatible nanofibrous scaffolds. Journal of biomaterials applications 33.10 (**2019**), 1327–1347. doi:10.1177/0885328219832984

[26] P. C. F. da Camara et al. Polyelectrolyte multilayers containing a tannin derivative polyphenol improve blood compatibility through interactions with platelets and serum proteins. Materials Science and Engineering: C 112 (**2020**), 110919. doi:10.1016/j.msec.2020.110919

[27] X. Man, J. Jin, B. Zhang, Surface modification of poly (propylene carbonate) by layer-by-layer assembly and its hemocompatibility. RSC Advances 4.73 (**2014**), 38943–38950. doi:10.1039/c4ra05982d

[28] Y. Liu et al., Layer by layer assembled phosphorylcholine groups on paclitaxel/chitosan nanofibers coatings for hemocompatibility improvement. Surface and Coatings Technology 357 (**2019**), 984–992. doi:10.1016/j.surfcoat.2018.10.074

[29] M. Kengo, H. Nara, Construction of stable biological albumin/heparin multilayers for elastic coatings on hydrophobic antithrombogenic artificial blood vessels. Tribology International 156 (**2021**), 106843. doi:10.1016/j.triboint.2020.106843

[30] M. Pandima Devi et al., A novel wound dressing material-fibrin-chitosan-sodium alginate composite sheet. Bulletin of Materials Science 35 (**2012**), 1157–1163. doi:10.1007/s12034-012-0404-5

[31] M. Castel-Molieres et al., Influence of homogenization technique and blend ratio on chitosan/alginate polyelectrolyte complex properties. Journal of Medical and Biological Engineering 38 (**2018**), 10–21. doi:10.1007/s40846-017-0304-7

[32] Y. Wang et al., A biomimetic silk fibroin/sodium alginate composite scaffold for soft tissue engineering. Scientific Reports 6.1 (**2016**): 39477

[33] D. Feng et al. Enhanced mechanical stability and sensitive swelling performance of chitosan/yeast hybrid hydrogel beads. New Journal of Chemistry 40.4 (**2016**), 3350–3362. doi:10.1039/c5nj02404h

[34] L. Jin et al. Effect of sodium alginate type on drug release from chitosan-sodium alginate–based in situ film-forming tablets. AAPS PharmSciTech 21 (**2020**), 1–9. doi:10.1208/s12249-019-1549-y

[35] Pankaj, Shashi Kishor, et al. Physicochemical characterization of plasma-treated sodium caseinate film. Food research international 66 (**2014**), 438–444. doi:10.1016/j.foodres.2014.10.016

[36] Z. Yang et al., Crystallization behavior of poly (ε-caprolactone)/layered double hydroxide nanocomposites. Journal of applied polymer science 116.5 (**2010**): 2658–2667. doi:10.1002/app

[37] A. M. Mohammed, J. M. Entidhar, Preparation and In-Vitro Evaluation of Clopidogrel Bisulfate Liquisolid Compact. Iraqi Journal of Pharmaceutical Sciences (P-ISSN 1683-3597 E-ISSN 2521-3512) (**2018**), 135–149. doi:10.31351/vol27iss2pp135-149

[38] A. Lowe et al. Effects of Emicizumab on APTT, FVIII assays and FVIII Inhibitor assays using different reagents: Results of a UK NEQAS proficiency testing exercise. Haemophilia 26.6 (**2020**), 1087–1091. doi:10.1111/hae.14177

[39] S. A. L. Ness, M. B. Brooks. Clotting times (aPTT and PT). Interpretation of Equine Laboratory Diagnostics (2017), 139–140. doi:10.1002/9781118922798.ch20

[40] D. M. Adcock, R. C. Gosselin, The danger of relying on the APTT and PT in patients on DOAC therapy, a potential patient safety issue. International Journal of Laboratory Hematology 39 (**2017**), 37–40. doi:10.1111/ijlh.12658

[41] N. F. Neamaha, AN Al-Jadaanb Shaker, M. A. Asmaa, Study of some of Novel Selena-Diazole Derivative activities on Hematological Parameters, Differentiate lymphocytes cells in addition to thyroid hormones levels in Female Rats (One of the series of studies on the impact of the new compound). Systematic Reviews in Pharmacy 11.11 (**2020**). doi:10.31838/srp.2020.11.140

[42] H. Ebrahim, F. Asrie, Z. Getaneh, Basic Coagulation Profiles and Platelet Parameters Among Adult Type 1 and Type 2 Diabetes Patients at Dessie Referral Hospital, Northeast Ethiopia: Comparative Cross-Sectional Study. J Blood Med. 12 (**2021**), 33–42. doi:10.2147/jbm.s287136

[43] M. A. Fadel et al. Dielectric properties and in vitro hemocompatibility of Nd: YAG laser-irradiated polyethylene terephthalate. Progress in Biomaterials 9 (**2020**), 107–114

[44] Q. He et al. Positive charge of chitosan retards blood coagulation on chitosan films. Journal of biomaterials applications 27.8 (**2013**), 1032–1045, doi:10.1177/0885328211432487

[45] Z. Hu, S. Lu, Y. Cheng et al. Investigation of the effects of molecular parameters on the hemostatic properties of chitosan. Molecules. 23 (2018) 12, 1–14. doi:10.3390/molecules23123147

[46] Fan, Lihong, et al. Synthesis and anticoagulant activity of sodium alginate sulfates. Carbohydrate polymers 83.4 (**2011**), 1797–1803.

[47] P. O. Kwiterovich Jr, Laboratory procedure manual: Total cholesterol, HDL-cholesterol, triglycerides, and LDL-cholesterol. National Health and Nutrition Examination Survey; Centers for Disease Control and Prevention: Atlanta, GA, USA (2004)

[48] S. Chinwong, D. Chinwong, A. Mangklabruks. Daily consumption of virgin coconut oil increases high-density lipoprotein cholesterol levels in healthy volunteers: a randomized crossover trial. Evidence-Based Complementary and Alternative Medicine 2017. doi:10.1155/2017/7251562

[49] H. Chen et al. Association between serum cholesterol levels and Alzheimer's disease in China: a case-control study. International Journal of Food Sciences and Nutrition 70.4 (**2019**), 405–411. doi:10.1080/09637486.2018.1508426

[50] L. Fernández-Friera et al. Normal LDL-cholesterol levels are associated with subclinical atherosclerosis in the absence of risk factors. Journal of the American College of Cardiology 70.24 (**2017**), 2979–2991. doi:10.1016/j.jacc.2017.10.024

[51] J. Hankins, The role of albumin in fluid and electrolyte balance. Journal of Infusion Nursing 29.5 (**2006**), 260–265.52

[52] A. Akirov, H. Masri-Iraqi, A. Atamna, I. Shimon, Low Albumin Levels Are Associated with Mortality Risk in Hospitalized Patients. Am J Med. 130 (2017) 12, 1465.e11–465.e19. doi:10.1016/j.amjmed.2017.07.020

[53] R. N. Moman, G. Nishant, M. Varacallo. Physiology, albumin. (2017)

[54] M. A. Jamiolkowski et al. An in vitro blood flow loop system for evaluating the thrombogenicity of medical devices and biomaterials. ASAIO journal 66.2 (**2020**), 183–189. doi:10.1097/MAT.0000000000000958

[55] K. Lau et al., Biomimetic silk biomaterials: Perlecan-functionalized silk fibroin for use in blood-contacting devices. Acta Biomaterialia 132 (**2021**), 162–175. Doi:10.1016/j.actbio.2021.02.014.

[56] J. M. Anderson, D. W. Grainger, S. W. Kim, Early events in blood/material interactions. Journal of Controlled Release 330 (**2021**), 31–35. doi:10.1016/j.jconrel.2020.11.023

[57] I. Cockerill et al. Designing better cardiovascular stent materials: A learning curve. Advanced functional materials 31.1 (**2021**), 2005361.doi:10.1002/adfm.202005361

[58] Y. Matsuhashi, K. Sameshima, Y. Yamamoto, M. Umezu, K. Iwasaki, Real-time visualization of thrombus formation at the interface between connectors and tubes in medical devices by using optical coherence tomography. PLoS ONE., 12 (2017) 12, 1–13. doi:10.1371/journal.pone.0188729

[59] R. Gbyli et al. Achieving totally local anticoagulation on blood contacting devices. Advanced Materials Interfaces 5.4 (**2018**), 1700954. .doi:10.1002/admi.201700954

[60] I. H. Jaffer et al. Medical device-induced thrombosis: what causes it and how can we prevent it? Journal of Thrombosis and Haemostasis 13 (**2015**), S72–S81. doi:10.1111/jth.12961

[61] M. Reinthaler, S. Braune, A. Lendlein, U. Landmesser, F. Jung, Platelets and coronary artery disease: Interactions with the blood vessel wall and cardiovascular devices. Biointerphases. 2016;11(2). doi:10.1116/1.4953246

[62] S. Braune et al. Evaluation of platelet adhesion and activation on polymers: Round-robin study to assess inter-center variability. Colloids and Surfaces B: Biointerfaces 158 (**2017**), 416–422. doi:10.1016/j.colsurfb.2017.06.053.

[63] L. Brancato et al. Surface nanostructuring of parylene-C coatings for blood contacting implants. Materials 11.7 (**2018**), 1109. doi:10.3390/ma11071109

[64] A. De Mel, K. Chaloupka, Y. Malam, A. Darbyshire, B. Cousins, A. M. Seifalian, A silver nanocomposite biomaterial for blood-contacting implants. J Biomed Mater Res - Part A., 100 (2012) A(9), 2348–2357. doi:10.1002/jbm.a.34177

[65] X. Tong, Z. Shi, L. Xu et al. Degradation behavior, cytotoxicity, hemolysis, and antibacterial properties of electro-deposited Zn–Cu metal foams as potential biodegradable bone implants. Acta Biomater., 102 (**2020**), 481–492. doi:10.1016/j.actbio.2019.11.031

[66] N. S. Merle, J. Leon, V. Poillerat et al. Circulating FH Protects Kidneys From Tubular Injury During Systemic Hemolysis. Front Immunol. 2020;11. doi:10.3389/fimmu.2020.01772

[67] V. Govindarajan, S. Zhu, R. Li et al. Impact of Tissue Factor Localization on Blood Clot Structure and Resistance under Venous Shear. Biophys J., 114 (**2018**) 4, 978–991. doi:10.1016/j.bpj.2017.12.034

[68] J. W. Kuhbier et al. Influence of direct or indirect contact for the cytotoxicity and blood compatibility of spider silk. Journal of Materials Science: Materials in Medicine 28 (**2017**), 1–9.doi:10.1007/s10856-017-5936-1

[69] G. Totea et al. In vitro hemocompatibility and corrosion behavior of new Zr-binary alloys in whole human blood. Open Chemistry 12.7 (**2014**), 796–803.doi:10.2478/s11532-014-0535-1

[70] M. Weber et al. Blood-contacting biomaterials: in vitro evaluation of the hemocompatibility. Frontiers in bioengineering and biotechnology 6 (**2018**), 99. doi:10.3389/fbioe.2018.00099